

CFTR fails to inhibit the epithelial sodium channel ENaC expressed in *Xenopus laevis* oocytes

G. Nagel¹, P. Barbry², H. Chabot³, E. Brochiero³, K. Hartung¹ and R. Grygorczyk³

¹Max-Planck-Institute of Biophysics, Max-von-Laue-Strasse 3, D-60438 Frankfurt am Main, Germany

²Institut de Pharmacologie Moléculaire et Cellulaire, CNRS UMR 6097, Sophia Antipolis, France

³Research Centre, Centre hospitalier de l'Université de Montréal - Hôtel-Dieu, 3850 Saint-Urbain, Montréal, Québec, Canada H2W 1T7

The cystic fibrosis transmembrane conductance regulator (CFTR) plays a crucial role in regulating fluid secretion by the airways, intestines, sweat glands and other epithelial tissues. It is well established that the CFTR is a cAMP-activated, nucleotide-dependent anion channel, but additional functions are often attributed to it, including regulation of the epithelial sodium channel (ENaC). The absence of CFTR-dependent ENaC inhibition and the resulting sodium hyperabsorption were postulated to be a major electrolyte transport abnormality in cystic fibrosis (CF)-affected epithelia. Several *ex vivo* studies, including those that used the *Xenopus* oocyte expression system, have reported ENaC inhibition by activated CFTR, but contradictory results have also been obtained. Because CFTR–ENaC interactions have important implications in the pathogenesis of CF, the present investigation was undertaken by our three independent laboratories to resolve whether CFTR regulates ENaC in oocytes and to clarify potential sources of previously reported dissimilar observations. Using different experimental protocols and a wide range of channel expression levels, we found no evidence that activated CFTR regulates ENaC when oocyte membrane potential was carefully clamped. We determined that an apparent CFTR-dependent ENaC inhibition could be observed when resistance in series with the oocyte membrane was not low enough or the feedback voltage gain was not high enough. We suggest that the inhibitory effect of CFTR on ENaC reported in some earlier oocyte studies could be attributed to problems arising from high levels of channel expression and suboptimal recording conditions, that is, large series resistance and/or insufficient feedback voltage gain.

(Received 11 November 2004; accepted after revision 28 February 2005; first published online 3 March 2005)

Corresponding author G. Nagel: Julius-von-Sachs-Institut, University Würzburg, Julius-von-Sachs-Platz 2, D 97082 Würzburg, Germany. Email: georg.nagel@botanik.uni-wuerzburg.de; and R. Grygorczyk: Research Centre, Centre hospitalier de l'Université de Montréal, Hôtel-Dieu, 3850 Saint-Urbain, Montréal, Québec, Canada H2W 1T7. Email: ryszard.grygorczyk@umontreal.ca

The primary function of the cystic fibrosis transmembrane conductance regulator (CFTR) is to mediate cAMP-activated anion (Cl⁻) conductance across the apical membrane of epithelial cells (Anderson *et al.* 1991; Nagel *et al.* 1992; Riordan, 1993; Gadsby *et al.* 1995; Quinton, 1999; Sheppard & Welsh, 1999; Dawson *et al.* 1999; Gadsby & Nairn, 1999; Nagel, 1999; Akabas, 2000). Consistent with its Cl⁻ channel function, disease-causing mutations in the CFTR gene result in impaired transepithelial Cl⁻ conductance, a hallmark of cystic fibrosis (CF) (Stutts & Boucher, 1999; Pilewski & Frizzell, 1999; Quinton, 1999). However, additional functions have been attributed to the CFTR, including regulation of the epithelial Na⁺ channel (ENaC) in airways and sweat glands (Stutts *et al.* 1995, 1997; Reddy *et al.* 1999; Reddy & Quinton, 2003), regulation of the outwardly rectifying Cl⁻ channel (Schwiebert *et al.* 1995, 1999), calcium-activated

Cl⁻ channel (Kunzelmann *et al.* 1997; Tarran *et al.* 2002) and ROMK2 potassium channel (McNicholas *et al.* 1997), vesicle trafficking (Bradbury *et al.* 1992), regulation of bicarbonate transport (Ko *et al.* 2002; Park *et al.* 2002) and the expression of inflammatory mediators (Donaldson & Boucher, 2003). These additional functions of the CFTR remain the subject of intense research and debate, while some earlier claims, such as CFTR-mediated ATP release (Reisin *et al.* 1994) or acidification of intracellular organelles (Barasch *et al.* 1991), have been questioned by later studies (Reddy *et al.* 1996; Bradbury, 1999).

Abnormal Na⁺ transport by CF-affected airway epithelia has been suggested by many *in vivo* and *in vitro* observations in humans and mice, showing increased amiloride-sensitive transepithelial potentials in CF (Knowles *et al.* 1981, 1983; Boucher *et al.* 1986;

Grubb *et al.* 1994; Mall *et al.* 1998; reviewed by Stutts & Boucher, 1999). The simplest interpretation of these early observations was that the rate of Na⁺ absorption was increased in CF, thereby explaining the dehydration of the airway surface liquid layer and the impaired clearance of pathogens. Na⁺ hyperabsorption was subsequently attributed to the absence of CFTR in the plasma membrane and to the lack of CFTR-dependent tonic inhibition of ENaC (Stutts *et al.* 1995, 1997). According to this hypothesis, loss of regulatory functions of CFTR is central to the development of CF pathology in the lungs. However, it is well established for human reabsorptive sweat ducts, where both the CFTR and the ENaC reside in the same apical membrane, that absence of the CFTR in CF-affected ducts does not elevate Na⁺ conductance (Bijman & Fromter, 1986), but under certain conditions may even significantly reduce it (Reddy *et al.* 1999; Reddy & Quinton, 2003). A direct relationship between ENaC and CFTR conductances in sweat ducts may not necessitate regulatory protein–protein interaction. As pointed out previously by Nagel *et al.* (2001*b*) and Horisberger (2003), due to an imposed Na⁺ concentration gradient in those experiments, at least part of the Na⁺ conductance reduction in CF-affected sweat ducts (Reddy *et al.* 1999) can arise from voltage-dependence of ENaC conductance, as predicted by the Goldman–Hodgkin–Katz equation (Hodgkin & Katz, 1949; Hille, 1992). Because CFTR activation induces a large voltage shift, Na⁺ current is then measured at a voltage where ENaC conductance is elevated (Nagel *et al.* 2001*b*). These observations in sweat glands are consistent with several studies in mouse lungs. First, Barbry & Lazdunski (1996) reviewed several studies on animal models describing an inactivation of CFTR which found no alteration of ion transport capacities in mouse airways. Second, Fang *et al.* (2002) identified the role played by the CFTR in the distal airspaces of the lung after stimulation of the cAMP cascade. Importantly, these authors clearly demonstrated that the presence or absence of functional CFTR did not affect basal lung liquid clearance, suggesting that the CFTR has no influence on ENaC activity in that tissue.

ENaC–CFTR interactions have been directly tested in several heterologous expression systems (Stutts *et al.* 1995, 1997). However, the most compelling demonstration of CFTR-dependent ENaC inhibition has come from studies on *Xenopus* oocytes co-expressing both channels. Significant reduction of macroscopic amiloride-sensitive Na⁺ current by cAMP-stimulated CFTR was reported by several research groups, including one of our laboratories (Mall *et al.* 1996; Briel *et al.* 1998; Chabot *et al.* 1999; Jiang *et al.* 2000; Ji *et al.* 2000; Suaud *et al.* 2002*a,b*). Assuming that specific protein–protein interactions were involved, the oocyte expression system was further used as

a functional assay in an attempt to identify regions on the CFTR or ENaC protein implicated in these interactions, but results obtained by different groups did not provide a consistent model (Schreiber *et al.* 1999; Jiang *et al.* 2000; Ji *et al.* 2000). In more recent studies, when series resistance was minimized (see below), ENaC inhibition by activated CFTR was often very small (<20%) or statistically insignificant (Suaud *et al.* 2002*a,b*; Samaha *et al.* 2004; Yan *et al.* 2004). A modified hypothesis suggested that CFTR-mediated changes of intracellular [Cl⁻] or Cl⁻ flux could inhibit ENaC (König *et al.* 2001). Published observations, however, are not unambiguous, for example Briel *et al.* (1998) stated that ENaC is inhibited in a voltage-dependent manner by Cl⁻ influx rather than by the cytosolic Cl⁻ concentration, whereas Konstas *et al.* (2003) found voltage-independent inhibition. König *et al.* (2001) attributed inhibition to the elevation of intracellular [Cl⁻], although this parameter was not measured directly in that study. In addition, a chloride-dependent inactivation mechanism would require tissue-specific regulation to explain the opposing effects observed in airways and sweat glands and is in contrast to the stimulation of ²²Na⁺ uptake by Cl⁻ influx in ENaC/CFTR-co-expressing oocytes (Nagel *et al.* 2001*b*).

Some recent studies did not find specific CFTR-dependent ENaC inhibition in MDCK epithelial cells or in *Xenopus* oocytes (Lahr *et al.* 2000; Nagel *et al.* 2001*b*). In particular, Nagel *et al.* (2001*b*) proposed that in *Xenopus* oocytes, under certain experimental conditions, apparent CFTR-dependent reduction of amiloride-sensitive current may be artefactual, a result of excessively large series resistance leading to considerable voltage-clamp errors. Because the resulting errors grow with increasing membrane conductance, activation of CFTR will reduce the fraction of voltage acting on the membrane. As a result, ENaC current is reduced due to a smaller electrical driving force, which could be misinterpreted as inhibition (Nagel *et al.* 2001*b*). This conclusion was supported by Chabot *et al.* (2002) in a recent erratum.

The aim of the present study was to determine whether cAMP activation of CFTR downregulates ENaC in *Xenopus* oocytes and to identify potential sources of dissimilar findings reported by different laboratories. The effect of CFTR activation on ENaC was examined in three independent laboratories, each with a different experimental protocol. We paid special attention to minimize voltage-clamp errors. Our three laboratories found no evidence of ENaC inhibition by activated CFTR if oocytes were voltage clamped with minimal series resistance and high feedback gain of the amplifier was used. Part of this study has been presented in preliminary form (Nagel *et al.* 2001*a*).

Methods

Electrophysiology

Two-electrode voltage-clamp experiments were performed with Turbo-Tec 05 (NPI Electronic, D-71732 Tamm, Germany), GeneClamp-500 (Axon Instruments, Union City, CA, USA) or TEV-200 voltage clamp (Dagan Corporation, Minneapolis, MN, USA) amplifiers (Chabot *et al.* 1999; Nagel *et al.* 2001*b*). Because membrane resistance (R_m) could be reduced significantly, sometimes even down to $\sim 1\text{ k}\Omega$ in oocytes expressing ENaC and/or CFTR (Nagel *et al.* 2001*b*; Nagel, 2004), special care was taken to keep other resistances in series with the membrane and between intra- and extracellular voltage-recording electrodes as low as possible. When R_m becomes comparable to the series resistance (R_s) of the recording circuit, only a fraction of the applied voltage will be experienced by the oocyte membrane, while the rest will drop across the R_s . Neglecting the R_s in such situations may lead to serious misinterpretation of the experimental data (Nagel *et al.* 2001*b*; Nagel, 2004). Therefore, the components contributing to R_s and the possibilities to reduce it are considered here in some detail (see also Hodgkin *et al.* 1952; Taylor *et al.* 1960; Armstrong & Gilly, 1992; Axon Instruments, 1993). In principle, any resistance in series with the membrane and between the electrodes measuring voltage across the membrane contributes to R_s (access resistance). Major sources to be considered are resistance of the cytoplasm, tissue covering the oocyte (e.g. the vitellin layer), the

electrolyte (bath) solution, agar bridges and Ag–AgCl electrodes. By careful design of the experiment, some of these elements may be eliminated, and resistance of others may be reduced. The remaining R_s can be compensated electronically, at least partially if necessary (Moore *et al.* 1984). Techniques to measure R_s have been described by Binstock *et al.* (1975). Generally, two electrodes, separate from the current-passing electrode, were used for differential membrane-potential measurements. Figure 1 presents schematic representations of the voltage-clamp arrangements employed here and the corresponding electrical circuits.

Voltage-clamp configuration

Membrane potential (V_m) is measured as the difference between an intracellular (V_{in}) and extracellular (V_{ref}) electrode with a high impedance differential amplifier ($V_m = V_{in} - V_{ref}$) in case of the Turbo-Tec 05 or Dagan amplifier. As with the Geneclamp 500 (Axon Instruments) differential measurement of the voltage is not possible, we used the arrangement suggested by Axon Instruments. A virtual ground amplifier (VG-2A) was used to measure current. This amplifier was connected to two bath electrodes, one to pass current and one to sense voltage, virtually without passing current. In all three cases, the extracellular electrode to measure V_m is placed, via an agar bridge, very close to the oocyte. The second bath electrode, used to pass current, is a Ag–AgCl wire.

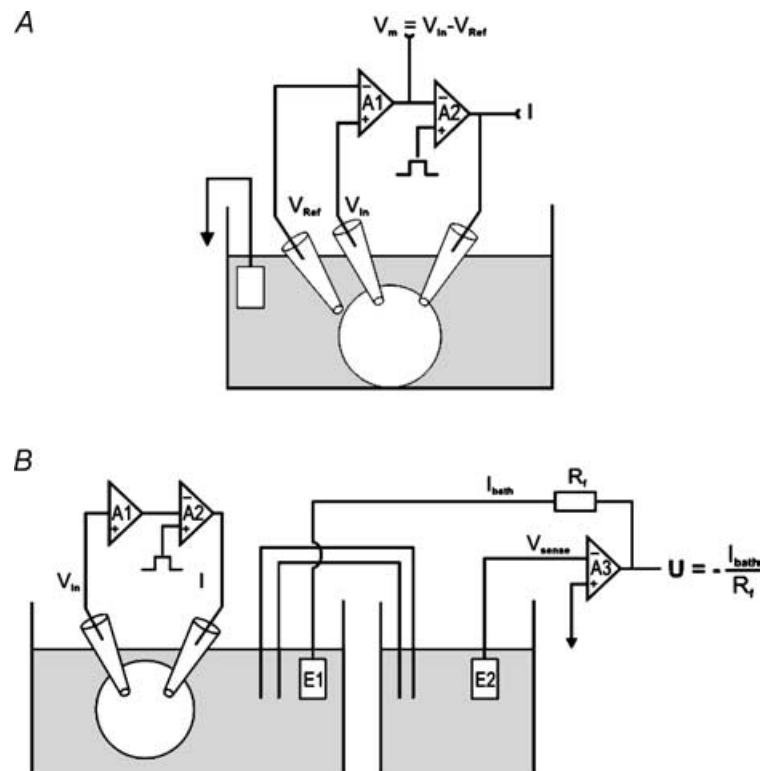


Figure 1. Schematic representation of different voltage-clamp configurations

Voltage-clamp arrangement as used with the Turbo-Tec (A) and the GeneClamp-500 (B) amplifier. See Methods for details.

Bath-fluid resistance was measured as described below and was typically close to 100 Ω when the external voltage-reference electrode (V_{ref}) was kept close to the oocyte (Nagel, 2004). This is in agreement with the calculated access resistance to a sphere of \varnothing 1 mm in ND96 solution (see below) (Hille, 1992; Baumgartner *et al.* 1999). However, R_s may increase up to several kiloOhms for some commercially available experimental chambers, which have a separate well for the bath electrode located at some distance from the oocyte (e.g. RC-10, Warner Instruments, Hamden, CT, USA).

Bath-fluid resistance measurements

Bath-fluid resistance of the recording chamber, an important part of the R_s in two-electrode voltage-clamp experiments (Nagel *et al.* 2001b; Nagel, 2004), could be estimated by the method described by Nagel (2004). Briefly, in the absence of an oocyte, the two glass microelectrodes that are normally used to impale the oocyte are introduced in the bath solution close to the position where an oocyte is normally placed. The external voltage reference electrode (a semi-microelectrode filled with KCl or an agar bridge) was placed close to the intracellular voltage electrode as in an experiment with an oocyte. In the set-up mode of the amplifier (current-clamp mode), the potential difference of the two microelectrodes to the reference was zeroed, and the amplifier was then switched to voltage clamp. The applied voltage was slowly increased until 10 μA of current was passing between the current-injecting electrode and the bath reference ground electrode. The voltage (in mV) required to drive 1 μA of current corresponds numerically to the combined R_s (in k Ω). With typical positions of the electrodes (i.e. the saline or agar bridge connecting to the reference electrode, as close as possible to the oocyte), a resistance of about 100 Ω was found between the voltage electrodes.

Determination of total R_s

To measure the total resistance in series with the membrane, current steps were applied and the resulting voltage drop was measured. Because the R_m is initially short-circuited by membrane capacity, the initial voltage drop is attributed to the resistance in series with the membrane.

Other sources of voltage-clamp errors

Insufficient feedback gain of the voltage-clamp amplifier is another source of voltage-clamp error which depends on the magnitude of membrane conductance. Under stationary voltage-clamp conditions, the difference between the command voltage and measured voltage depends on the R_m , the gain of the feedback amplifier and the resistance of the current electrode plus the output

resistance of the amplifier (see e.g. Axon Instruments, 1993):

$$V = V_{\text{cmd}} \alpha K / (\alpha K + 1) \text{ with } K = R_m / (R_m + R_{\text{in}} + R_{\text{out}})$$

where V_{cmd} is the command voltage, α is the feedback gain of the amplifier, R_m is the resistance of the cell membrane, R_{in} is the resistance of the current-injecting electrode, and R_{out} the output resistance of the voltage clamp amplifier.

To give an example: with a feed back gain of 1000, $R_m = 5000 \Omega$, $R_{\text{in}} = 0.5 \text{ M}\Omega$ plus output resistance of the voltage clamp amplifier (1 $\text{M}\Omega$, e.g. the HS-2Ax10 headstage of Axon), the stationary voltage error is 23%. Increasing the R_m to 10 k Ω decreases the error to 13%. In contrast to errors due to R_s this type of error can be recognized by monitoring the measured V_m and comparing it with the command voltage. It is possible to correct the error by increasing the feedback gain although this is not always feasible because the voltage-clamp circuit has a tendency to oscillate at high gains. The interesting point here is that an elevation of membrane conductance, for example CFTR activation, will increase the voltage error and decrease the driving force on total conductance. Thus, with low feedback gain, activation of the CFTR could result in an apparent decrease of amiloride-sensitive ENaC conductance, which could be misinterpreted as the result of interaction between the two channels.

Oocyte acquisition and injection

Oocyte isolation and injection procedures were described in previous publications from our laboratories (Weinreich *et al.* 1997, 1999; Chabot *et al.* 1999). Mature female *Xenopus laevis* were maintained at 18–20°C with a 12-h light–dark cycle. Oocyte clusters were surgically removed from the ovaries and torn apart with forceps in ND96 medium containing (mM): NaCl 96, KCl 2, Hepes 10, CaCl₂ 1.8; at pH 7.4. Denuded oocytes were obtained by collagenase digestion (type IA, 370 U ml⁻¹, Sigma) for 2 h at room temperature and rinsed several times in ND96 or ORi solutions (see below). Stage 5–6 oocytes were selected and incubated overnight at 18°C in ND96 or ORi medium with gentamycin (50 $\mu\text{g ml}^{-1}$). Healthy oocytes were selected and injected with up to 50 nl cRNA (5–200 ng μl^{-1}). The oocytes were incubated for 2–4 days after injection in ND96 or ORi medium supplemented with gentamycin and 10 $\mu\text{mol l}^{-1}$ amiloride.

Solutions

The ND96 solution contained (mM): NaCl 96, KCl 2, MgCl₂ 1, Hepes 5, sodium pyruvate 2.5 and CaCl₂ 1.8; and 40 U ml⁻¹ penicillin, 40 $\mu\text{g ml}^{-1}$ streptomycin and 50 mg l⁻¹ gentamycin; at pH 7.6. The ORi solution contained (mM): NaCl 110, KCl 5, CaCl₂ 2, MgCl₂ 1.8 and Mops 5; at pH 7.6.

Experimental protocols

Two different experimental protocols were followed to study the effect of CFTR activation on ENaC co-expressed in oocytes. Protocol 1 (data in Fig. 2): oocytes were kept under open-circuit conditions except for short periods (< 30 s) during which they were voltage clamped, and the voltage-ramp protocol (V from -150 mV to $+100$ mV in

10 s) was applied to determine the current–voltage (I – V) relationship. A fast perfusion system allowed complete change of the bath solution within less than 10 s. The following solutions were applied sequentially to the oocyte during an experiment to measure ENaC and CFTR current (Protocol 1, Table 1, data in Fig. 2): A1, ND96 + $10 \mu\text{M}$ amiloride; B, ND96; A2, ND96 + $10 \mu\text{M}$ amiloride;

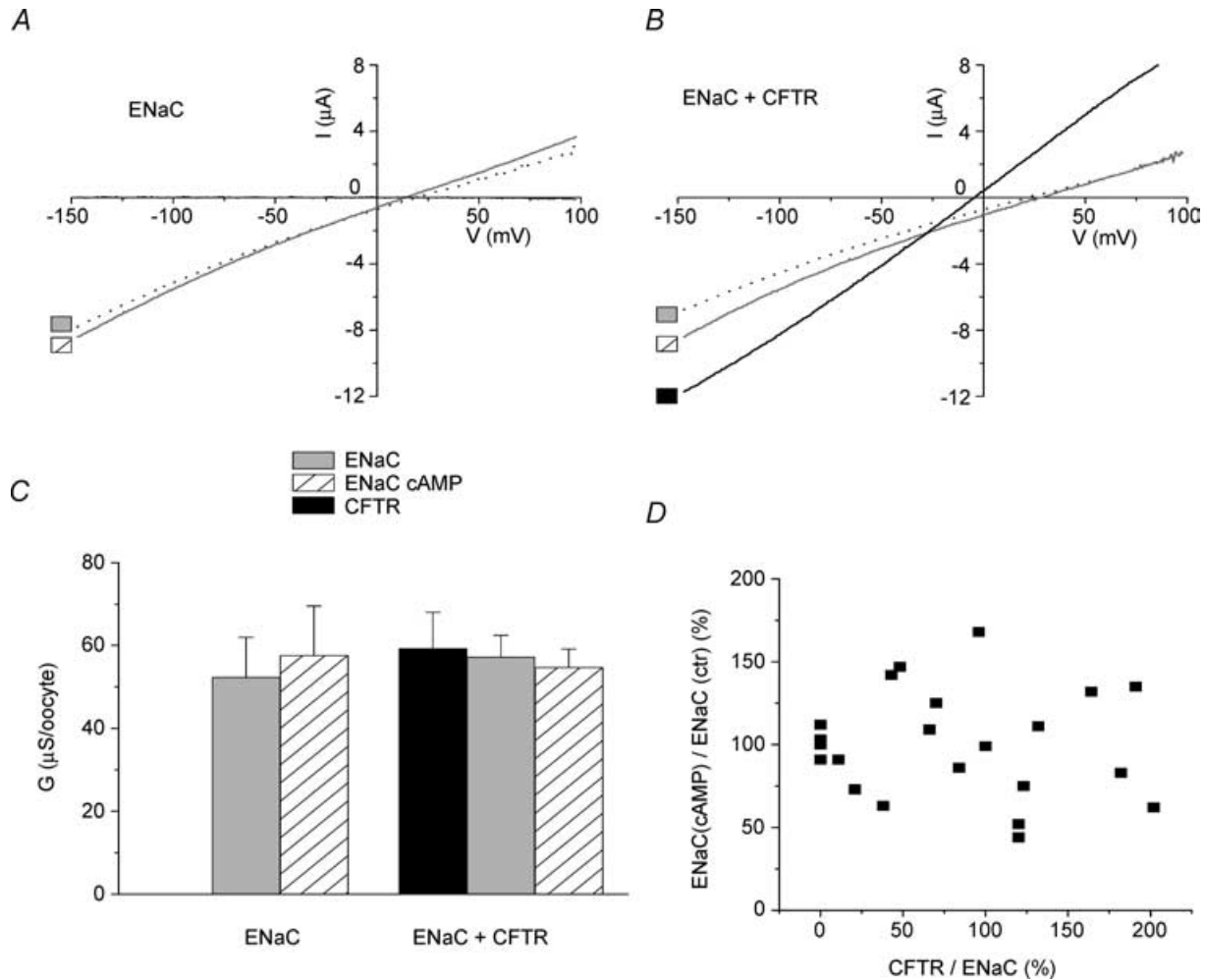


Figure 2. Human ENaC is not regulated by the human CFTR co-expressed in *Xenopus* oocytes

A, representative current–voltage (I – V) relationships obtained with an oocyte expressing human α -, β - and γ -ENaC only. Specific amiloride-sensitive ($10 \mu\text{M}$), ENaC-mediated current is shown in response to a voltage ramp (see Methods). The two lines represent the I – V relationship before (dotted line), and after application of cAMP-elevating cocktail (see Methods, continuous grey line). Note the lack of effect of cAMP elevation on ENaC-mediated current. B, representative I – V relationships obtained with an oocyte co-expressing hENaC and hCFTR. The graph shows specific amiloride-sensitive, ENaC-mediated current before and after the application of a cAMP-elevating cocktail, dotted and continuous grey lines, respectively. The continuous black line represents cAMP-stimulated, CFTR-mediated current measured in the presence of amiloride. Note that in the presence of the CFTR, elevation of cAMP had no significant (NS) effect on the slope of ENaC-mediated current, although its reversal potential was slightly, but statistically significantly, increased (change in $V_r = 13$ mV, $P < 0.001$). C, summary of results: conductances G_{CFTR} , G_{ENaC} and $G_{\text{ENaC(cAMP)}}$ were calculated from the slopes of the I – V relationships such as those shown in A and B. The difference between the number of oocytes measured in the presence of the CFTR ($n = 19$) and the number of oocytes measured in the absence of the CFTR ($n = 4$) is due to the fact that only oocytes exhibiting similar levels of ENaC conductance were presented here (four oocytes), but cAMP insensitivity was also noticed in oocytes exhibiting higher levels of conductance (see D below). D, effect of CFTR activation on ENaC-mediated conductance in oocytes expressing different $G_{\text{CFTR}}/G_{\text{ENaC}}$ ratios. The graph shows relative change of ENaC-mediated conductance $G_{\text{ENaC(cAMP)}/G_{\text{ENaC}}$ in each individual oocyte measured before and after CFTR activation. The figure illustrates that CFTR activation had no effect on the hENaC at $G_{\text{CFTR}}/G_{\text{ENaC}}$ ratios up to 2.

Table 1. Solutions used in experiments shown in Fig. 2

Solution	ENaC activated	CFTR activated
A1	–	–
A2	–	–
B	+	–
C1	–	+
C2	–	+
D	+	+

Effect of solutes on ENaC and CFTR conductance. Activity (+) and lacking activity on inhibition (–) of the CFTR or ENaC conductance, respectively, are indicated.

C1, ND96 + 10 μM amiloride + 10 μM forskolin + 100 μM 8-(4-chlorophenylthio)cAMP (cpt cAMP) + 100 μM 3-isobutyl-1-methylxanthine (IBMX); D, ND96 + 10 μM forskolin + 100 μM cpt cAMP + 100 μM IBMX; C2, ND96 + 10 μM amiloride + 10 μM forskolin + 100 μM cpt cAMP + 100 μM IBMX. The specific control ENaC current was determined as: $B - \frac{1}{2}(A1 + A2)$. The specific ENaC current in cAMP-stimulated oocytes was determined as: $D - \frac{1}{2}(C1 + C2)$. The specific CFTR current was determined as $\frac{1}{2}[(C1 + C2) - (A1 + A2)]$. Protocol 2 (data in Fig. 3): oocytes were voltage clamped at -60 mV, and membrane current was recorded continuously. The specific control ENaC current was determined as the average of the amiloride-sensitive (10 μM amiloride) current before stimulation with 1 mM IBMX at the beginning of an experiment and after washout of IBMX at the end of that experiment. The specific ENaC current in the presence of activated CFTR was determined as amiloride-sensitive current after full activation of CFTR with 1 mM IBMX. The specific CFTR current was determined as amiloride-insensitive, IBMX-stimulated current.

Results

CFTR fails to inhibit human and rat ENaC co-expressed in *Xenopus* oocytes

Figure 2A shows the I – V relationships of amiloride-sensitive current in oocytes expressing the α -, β - and γ -subunits of human ENaC (hENaC). It demonstrates that amiloride-sensitive, hENaC-mediated current was not affected by cAMP stimulation. When the hENaC was co-expressed with the human CFTR (hCFTR), application of cAMP-elevating cocktail to these oocytes activated a large CFTR-mediated current, but had no effect on amiloride-sensitive current (Fig. 2B). Figure 2C summarizes whole-cell ENaC- and CFTR-mediated conductances (G_{ENaC} and G_{CFTR} , respectively) calculated from the slope of the I – V relationships, such as those shown in Fig. 2A and B. Mean G_{ENaC} was not different

in oocytes expressing ENaC alone and those co-expressing CFTR in the absence of cAMP stimulation. Furthermore, in the latter group of oocytes, G_{ENaC} was also not affected by cAMP stimulation of the CFTR. Thus, our results provide no evidence of the negative regulation of hENaC by the CFTR. As ENaC inhibition may require higher expression levels of G_{CFTR} relative to G_{ENaC} , we have examined oocytes expressing different $G_{\text{CFTR}}/G_{\text{ENaC}}$ ratios (Fig. 2D). This figure shows that even at $G_{\text{CFTR}}/G_{\text{ENaC}}$ ratios of ~ 2 , stimulation of CFTR had no effect on hENaC activity.

In an independent study, the α -, β - and γ -subunits of rat ENaC (rENaC) were expressed instead of hENaC (Fig. 3). In this study, a different experimental protocol was used (i.e. oocytes co-expressing rENaC and CFTR were voltage clamped at a fixed V_m of -60 mV) and the oocyte current was recorded continuously during the entire experiment. Figure 3A gives an example of a current trace from such an experiment performed without compensating the R_s of the bath fluid and the ground electrode. Elevation of intracellular cAMP by including 1 mM IBMX in the perfusate resulted in significant stimulation of CFTR-mediated current, and, under these conditions, an apparent reduction of amiloride-sensitive, ENaC-mediated current. However, when the R_s was reduced by using the virtual ground bath amplifier with two bath electrodes, no inhibition of amiloride-sensitive current was observed (Fig. 3B). This demonstrates that apparent inhibition of the ENaC by the CFTR may inadvertently occur if the R_s is not properly reduced. Figure 3C summarizes the data from several experiments, such as those in Fig. 3B, showing that CFTR activation had no statistically significant effect on rENaC. Figure 3D examines this effect in oocytes expressing different CFTR/ENaC current ratios and reveals that even at ratios approaching 4, the CFTR did not inhibit rENaC. Thus, our results with hENaC and rENaC confirm the previous report by Nagel *et al.* (2001b) that the CFTR does not inhibit the ENaC in oocytes, if oocyte V_m is properly controlled.

In a further series of voltage-clamp experiments with rENaC/h CFTR-co-expressing oocytes, we examined the effect of the feedback gain (voltage gain) on apparent ENaC conductance and its apparent ‘regulation’ by activated CFTR. In these experiments, the actual membrane voltage was also measured, but the observed voltage deviations from the target value at the different gains (see Methods: ‘Other sources of voltage-clamp errors’) were not taken into account when calculating ‘apparent conductances’, as is usually done by all commercial software. In addition, we determined real conductances from the actually observed current and voltage values. Table 2 shows both apparent and real ENaC conductances before and after CFTR activation, determined at three different voltage gains. As expected, lower voltage gain leads to a decreased

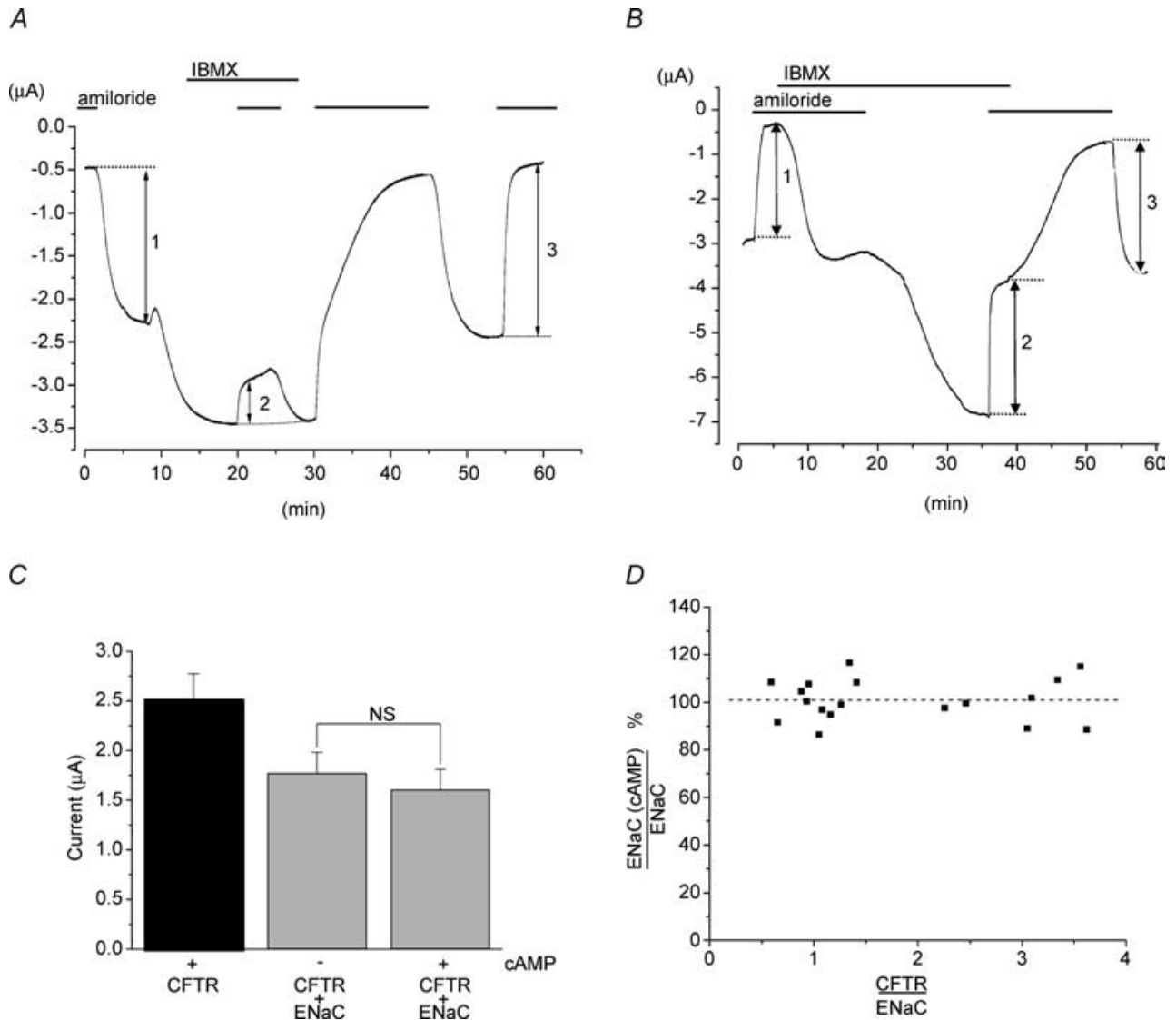


Figure 3. Rat ENaC is not regulated by the human CFTR co-expressed in *Xenopus* oocytes

A, example of a current trace recorded at -60 mV from an oocyte co-expressing α -, β - and γ -rENaC and hCFTR recorded with a single bath electrode (see Fig. 1; i.e. relatively large R_s of about 6 k Ω ; see below). Horizontal lines indicate the application of 10 μ M amiloride to block the ENaC or 1 mM IBMX to stimulate the CFTR. Vertical arrows indicate the amplitudes of ENaC-mediated, amiloride-sensitive Na^+ current (I_{ENaC}) observed before, during and after IBMX stimulation, arrows 1, 2 and 3, respectively. Note that CFTR stimulation, seen as increased inward current during IBMX application, resulted in apparent inhibition of amiloride-sensitive current (compare vertical arrow 2 with 1 or 3). The bath-fluid resistance of the experimental chamber (RC-10, Warner Instruments Co) filled with ND96 solution was ~ 4.5 k Ω , the combined resistance of the reference bath electrode and the agar bridge was ~ 1.5 k Ω . B, an example of an experiment similar to A, but performed with the virtual ground amplifier connected with two electrodes to the bath to reduce R_s (cf. Fig. 1). No reduction of ENaC current by the CFTR was observed under these conditions; compare the inhibition of ENaC by amiloride in the presence of activated CFTR (arrow 2) with that before (arrow 1) and after CFTR deactivation (arrow 3). C, summary of ENaC-mediated and CFTR-mediated currents measured with low R_s as in B, filled bar, I_{CFTR} ; grey bars, I_{ENaC} without (left) and with (right) stimulation of the CFTR by IBMX. Oocytes were clamped at the holding potential of -60 mV. The data are means \pm s.e.m., $n = 23$. The observed ENaC current amplitudes were not statistically significantly different (NS) before and after CFTR stimulation. D, effect of activated CFTR on I_{ENaC} observed in oocytes expressing different ratios of I_{CFTR}/I_{ENaC} . Oocytes were voltage-clamped at -60 mV and stimulated with 1 mM IBMX. The slope of the linear regression fitted to the data points was not significantly different from 0 ($P = 0.99$, $n = 18$ oocytes from seven different frogs).

Table 2. Apparent and real ENaC conductances (in μS) in rENaC/hCFTR-co-expressing oocytes measured with three different voltage gains

Voltage gain	No CFTR activation		Full CFTR activation	
	G_{app}	G_{real}	G_{app}	G_{real}
1 k	55	62	25	67
4 k	62	65	52	68
10 k	61	62	59	68

In this example 2.8 ng rENaC-cRNA and 0.8 ng hCFTR-cRNA were injected and oocyte conductance was measured after 50 h of incubation; representative of four other experiments with low cRNA amounts. CFTR was activated by 0.5 mM IBMX + 10 μM forskolin. Apparent conductance (G_{app}) was determined as the current slope between -20 mV and $+20$ mV and real conductance (G_{real}) was determined as the current slope between the actually observed voltages, with -20 mV and $+20$ mV as target values in the voltage clamp protocol. Both G_{app} and G_{real} are given in μS . Configuration as in Fig. 1B with two bath electrodes and an estimated R_s of less than 200 Ω . Although in this example G_{real} is slightly larger during CFTR activation, ENaC seems significantly inhibited by CFTR activation when compared to G_{app} , obtained at a voltage gain of 1 k.

apparent ENaC conductance when the CFTR is activated, and this directly results from voltage-clamp errors (see Methods: 'Other sources of voltage clamp errors').

To demonstrate that CFTR activation modulates the amiloride-sensitive component of the V_m , we measured V_m under current-clamp conditions (with $I = 0$) before and after CFTR stimulation. Amiloride was briefly removed (to activate ENaC conductance), and corresponding shifts of V_m were measured. Figure 4A shows the voltage shift induced by amiloride removal in hCFTR/rENaC-co-expressing oocytes before and after CFTR activation. Clearly, the amiloride-induced voltage shift was much smaller, once the CFTR was activated. The effect of CFTR activation on the amiloride-sensitive voltage shift was fully reversible, as demonstrated in Fig. 4B, where amiloride removal-induced voltage shift was examined first with activated CFTR and then after CFTR inactivation. The mean amiloride-sensitive voltage shift for rENaC/hCFTR-co-expressing oocytes was 35 ± 7 mV with CFTR inactive and dropped to 10 ± 5 mV after CFTR activation ($n = 8$). This effect was not specific for CFTR-mediated conductance, because non-specific increase of membrane conductance introduced, for example by simply rupturing the oocyte membrane, also decreased the ENaC-related, amiloride-sensitive voltage shift (data not shown). It is important to note that for each oocyte tested in these current-clamp experiments, we also confirmed that ENaC conductance was not influenced by CFTR activation under voltage-clamp conditions with high voltage gain and low R_s . Although this might seem paradoxical at first glance, modulation of the amiloride-induced voltage shift by other conductances is in fact expected and will be explained in the Discussion.

Discussion

The hypothesis that the CFTR inhibits the ENaC has its roots in early studies before the involved channels, the CFTR and the ENaC, were identified at the molecular level. *In vivo* and *in vitro* transepithelial potential measurements on normal and CF-affected airway epithelia detected increased amiloride sensitivity of CF-affected tissues (Knowles *et al.* 1981, 1983). This was attributed to increased rates of Na absorption (hyperabsorption) by CF-affected epithelia and seemed to explain elegantly the abnormally dehydrated mucus in CF-affected airways (Boucher *et al.* 1986). After cloning the CFTR and ENaC (Riordan *et al.* 1989; Canessa *et al.* 1993; Lingueglia *et al.* 1993), it was expected that one of the functions of the CFTR was to inhibit the ENaC (Stutts *et al.* 1995). Indeed, several laboratories subsequently reported direct inhibition of the ENaC by the CFTR in several experimental systems, including voltage-clamped oocytes of *Xenopus laevis* (Mall *et al.* 1996; Letz & Korbmayer, 1997; Jiang *et al.* 2000; Saud *et al.* 2002a,b; Konstas *et al.* 2003). Our present results demonstrate that the CFTR does not inhibit ENaC in oocytes and are thus in direct contrast to previous reports, which used the same expression system. This could not be attributed to low expression ratios of the CFTR compared to the ENaC (Kunzelmann, 2003), because we have examined the effect at different CFTR/ENaC conductance ratios (up to 4, absolute conductance ranges were 10–100 μS for the ENaC and 10–300 μS for the CFTR) and under widely varying conditions. Furthermore, we found no inhibitory effect with both hENaC and rENaC (Fig. 2D and 3D; and Nagel *et al.* 2001b). It was also suggested that functional ENaC–CFTR interactions may differ between murine and human ENaC, as well as, that they could be influenced by naturally occurring polymorphism of α -hENaC (Yan *et al.* 2004). They found less than 35% inhibition of murine ENaC by activated CFTR (their Fig. 1A), only a modest 20% inhibition for wildtype α -hENaC and no change for T663A α -hENaC, where threonine 663 (wildtype) was replaced by alanine (their Fig. 2). Because in these recent experiments Yan *et al.* (2004) also used a virtual ground, as in our experiments, voltage-clamp errors could be avoided if experiments were performed at high voltage gain and with low series resistance. Thus, the absence or negligible inhibition is expected and agrees with our data. Indeed, in our present study we used the same variant T663 for which Yan *et al.* (2004) found a modest inhibition (20%, their Fig. 2), whereas we found no inhibition when R_s was fully compensated and high gain of the amplifier was used.

As our three laboratories did not observe ENaC inhibition by CFTR activation, the obvious question arises: how to reconcile our findings with those reported by other investigators? After careful examination of all the different experimental conditions, we come to the conclusion that

the only reasonable explanation for such divergent results is the way the two-electrode voltage-clamp techniques were deployed. For example, high R_s or too low feedback voltage gain could both limit the ENaC conductance measured. Because an R_s problem can arise easily and inadvertently, and indeed it happened to one of us (Chabot *et al.* 1999, 2002), we made an effort to closely examine the problem and to find a simple method to estimate the actual R_s of the recording setup. As recently demonstrated by one of us (Nagel *et al.* 2001*b*), the R_s in the measuring circuit may simulate ENaC inhibition if the R_m drops due to activation of large membrane conductance (Nagel *et al.* 2001*b*; Nagel, 2004; see also Fig. 3*A*). This hypothesis is further strengthened by closely examining experimental data published by other laboratories. For example, König *et al.* (2001) reported ENaC inhibition

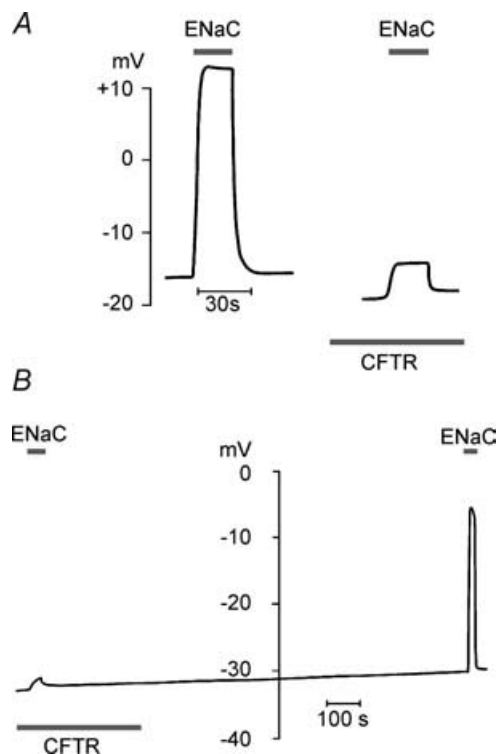


Figure 4. Amiloride-induced voltage shift is modulated by membrane conductance changes

A, when the hCFTR is inactive, rENaC activation by removal of amiloride (indicated by the bar labelled ENaC) depolarizes an oocyte in this example from -16 mV to $+13$ mV. Activation of the CFTR (by 0.5 mM IBMX + 10 μ M forskolin, indicated by the bar labelled CFTR) yields slight hyperpolarization (to -19 mV), and subsequent activation of ENaC depolarizes the oocyte to only -14 mV. The trace shown is representative of seven similar experiments in which voltage-clamp measurements showed that ENaC conductance is not affected by CFTR activation. *B*, continuous voltage recording from another hCFTR/rENaC-co-expressing oocyte, where CFTR and ENaC were activated in a reversed order compared to *A* (i.e. CFTR was activated first, at the beginning of the experiment, and then inactivated). The data show increase of ENaC-related, amiloride-induced voltage shift after inactivating CFTR (washout of IBMX/forskolin), demonstrating reversibility of the effect.

by the CFTR and intracellular Cl^- . However, under their experimental conditions, the ENaC was not only inhibited by activation of a completely unrelated chloride channel, ClC-0 , but also by permeabilization of the membrane with amphotericin. Thus, all manoeuvres that increased membrane conductance – expression of the CFTR or ClC-0 or amphotericin-induced membrane permeabilization – resulted in apparent ENaC inhibition. To us, these data suggest that the R_s probably limits the measurable conductance and, in this way, simulates ENaC ‘inhibition’. In addition, apparent ENaC inhibition could result when too low gain in the voltage feedback loop is used, once additional conductance is activated (see Table 2). Other groups recently studied ENaC–CFTR interactions in oocytes that were voltage clamped with a presumably low R_s . However, their actual data show that cAMP stimulation of wild-type CFTR had a very small ($< 20\%$) or statistically non-significant effect on the ENaC (Suaid *et al.* 2002*a,b*; Yan *et al.* 2004). Such results are expected if oocytes were clamped with minimal R_s and, thus, are consistent with our interpretation.

The assumption that the apparent interaction between the CFTR and ENaC is due to voltage-clamp errors explains a variety of observations reported in the literature. First, it explains why the CFTR seems to interact with almost all other electrogenic transport systems – channels as well as transporters. Second, it explains that the degree of inhibition depends on the expression level, i.e. the CFTR-mediated conductance. Third, it also explains the results of mutation experiments if one takes into account that the conductances induced by mutated CFTR channels are much lower (Mall *et al.* 1996; Briel *et al.* 1998; Schreiber *et al.* 1999) and fourth, it explains why the reduction of Cl^- concentration, and therefore membrane conductance, reduces the apparent interaction between the CFTR and ENaC.

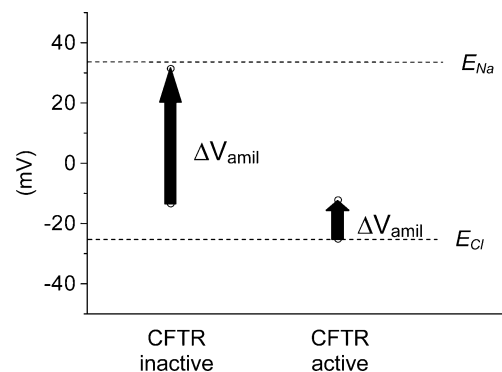


Figure 5. Amiloride-induced voltage shifts in oocytes expressing ENaC and CFTR

The diagram shows predicted membrane voltage shifts induced by amiloride removal (ΔV_{amil} , vertical arrows) for oocytes under current-clamp condition with CFTR inactive or after CFTR activation. ΔV_{amil} was calculated as described in the Discussion. E_{Na} and E_{Cl} (dashed lines) represent Nernst potentials for Na^+ and Cl^- , respectively.

It might be also interesting to review the early findings of elevated amiloride-induced voltage shifts in CF-affected tissues which ultimately led to the notion of increased sodium absorption in CF. In fact, we also observed similar effects in CFTR/ENaC-co-expressing oocytes. As Fig. 4 shows, the amiloride-induced voltage shift is smaller once the CFTR is activated. It is often assumed that such reduction of *voltage* shift hints of CFTR-dependent inhibition of amiloride-sensitive sodium *current*. However, this is not necessarily the case and alternative explanations are possible. In the following example, we will consider amiloride-induced voltage shifts in oocytes expressing the CFTR and ENaC. V_m can be well described by the Goldman–Hodgkin–Katz equation:

$$V_m = RT/F \times \ln \frac{P_K[K^+]_o + P_{Na}[Na^+]_o + P_{Cl}[Cl^-]_i}{P_K[K^+]_i + P_{Na}[Na^+]_i + P_{Cl}[Cl^-]_o} \quad (1)$$

where $[Cl^-]_i = 45$ mM, $[Na^+]_i = 30$ mM and $[K^+]_i = 120$ mM, and $[Cl^-]_o = 121$ mM, $[Na^+]_o = 110$ mM and $[K^+]_o = 5$ mM. As an illustration, let us assume that $P_K = 0.01 \times P_{Na}$ and that in the absence of CFTR stimulation, the residual $P_{Cl} = 0.01 \times P_{Na}$, while after CFTR activation, $P_{Cl} = 3 \times P_{Na}$. Also, let us assume that in the presence of amiloride, residual $P_{Na} = 0.01 \times P_{Na}$ and then calculate V_m for different experimental situations. With the CFTR inactive and amiloride present, $V_m = -13.5$ mV, while upon amiloride removal, it will increase to $+31.4$ mV. After CFTR stimulation and in the presence of amiloride, V_m will be -25.2 mV, whereas with active CFTR and ENaC, the V_m will be -12.2 mV.

Thus, the amiloride-induced voltage shift when the CFTR is inactive will be ~ 45 mV, while it will be much smaller after CFTR activation: 13 mV (see Fig. 5). Indeed, this confirms qualitatively what we observed in voltage measurements on CFTR/ENaC-co-expressing oocytes (Fig. 4). The experimentally observed values are slightly different because the actual conductances and intracellular ion concentrations may be somewhat different from those used in our simple example. Not surprisingly, activation of a chloride conductance, which is not mediated by the CFTR, may also lead to a reduced amiloride-induced voltage shift in transepithelial voltage measurements, without the need to invoke 'regulatory interactions' as is done often (e.g. Schreiber *et al.* 2003). Of course, this argument does not apply to careful conductance estimates derived from application of current injections. Conductance measurements by current injections can, under certain conditions, accurately reflect amiloride-sensitive sodium conductance. Such conductance measurements will, however, only yield reliable results if residual conductance is not overwhelming and if R_s is not too large. It is also important to stress that our study is limited to only one expression system,

amphibian oocytes. It may well be that CFTR–ENaC regulatory interactions cannot be reproduced in oocytes because some factor(s), which are required for such interactions, are missing in these cells. Thus, it will be critical to extend our study to other cellular systems, while ensuring optimal recording conditions.

In summary, the results from our three independent laboratories univocally demonstrated the absence of ENaC inhibition by the CFTR in *Xenopus* oocytes, when R_s of the recording circuitry was low ($\sim 100 \Omega$). We suggest that the inhibitory effects previously reported in the literature could be attributed to either unfavourably large R_s or insufficient voltage gain or both, resulting in apparent reduction of ENaC conductance. Lessons from the oocyte expression system argue for careful re-examination of other *in vitro* experimental systems in which CFTR–ENaC regulatory interactions are studied, especially in whole-cell patch-clamp experiments, where it is known that access resistance has to be monitored carefully (Armstrong & Gilly, 1992).

References

- Akabas MH (2000). Cystic fibrosis transmembrane conductance regulator. Structure and function of an epithelial chloride channel. *J Biol Chem* **275**, 3729–3732.
- Anderson MP, Berger HA, Rich DP, Gregory RJ, Smith AE & Welsh MJ (1991). Nucleoside triphosphates are required to open the CFTR chloride channel. *Cell* **67**, 775–784.
- Armstrong CM & Gilly WF (1992). Access resistance and space clamp problems associated with whole-cell patch clamping. *Methods Enzymol* **207**, 100–122.
- Axon Instruments (1993). The Axon Guide pp. 1–282. Axon Instruments Inc., Foster City, CA.
- Barasch J, Kiss B, Prince A, Saiman L, Gruenert D & al Awqati Q (1991). Defective acidification of intracellular organelles in cystic fibrosis. *Nature* **352**, 70–73.
- Barbry P & Lazdunski M (1996). Structure and regulation of the amiloride-sensitive epithelial sodium channel. *Ion Channels* **4**, 115–167.
- Baumgartner W, Islas L & Sigworth FJ (1999). Two-microelectrode voltage clamp of *Xenopus* oocytes: voltage errors and compensation for local current flow. *Biophys J* **77**, 1980–1991.
- Bijman J & Fromter E (1986). Direct demonstration of high transepithelial chloride-conductance in normal human sweat duct which is absent in cystic fibrosis. *Pflugers Arch* **407** (Suppl. 2), S123–S127.
- Binstock L, Adelman WJ, Senft P, Jr & Lecar H (1975). Determination of the resistance in series with the membranes of giant axons. *J Membr Biol* **21**, 25–47.
- Boucher RC, Stutts MJ, Knowles MR, Cantley L & Gatzky JT (1986). Na^+ transport in cystic fibrosis respiratory epithelia. Abnormal basal rate and response to adenylate cyclase activation. *J Clin Invest* **78**, 1245–1252.
- Bradbury NA (1999). Intracellular CFTR: localization and function. *Physiol Rev* **79**, S175–S191.

- Bradbury NA, Jilling T, Berta G, Sorscher EJ, Bridges RJ & Kirk KL (1992). Regulation of plasma membrane recycling by CFTR. *Science* **256**, 530–532.
- Briel M, Greger R & Kunzelmann K (1998). Cl⁻ transport by cystic fibrosis transmembrane conductance regulator (CFTR) contributes to the inhibition of epithelial Na⁺ channels (ENaCs) in *Xenopus* oocytes co-expressing CFTR and ENaC. *J Physiol* **508**, 825–836.
- Canessa CM, Horisberger JD & Rossier BC (1993). Epithelial sodium channel related to proteins involved in neurodegeneration. *Nature* **361**, 467–470.
- Chabot H, Vives MF, Dagenais A, Grygorczyk C, Berthiaume Y & Grygorczyk R (1999). Downregulation of epithelial sodium channel (ENaC) by CFTR co-expressed in *Xenopus* oocytes is independent of Cl⁻ conductance. *J Membr Biol* **169**, 175–188.
- Chabot H, Vives MF, Dagenais A, Grygorczyk C, Berthiaume Y & Grygorczyk R (2002). Downregulation of epithelial sodium channel (ENaC) by CFTR co-expressed in *Xenopus* oocytes is independent of Cl⁻ conductance – Erratum. *J Membr Biol* **186**, 185.
- Dawson DC, Smith SS & Mansoura MK (1999). CFTR: mechanism of anion conduction. *Physiol Rev* **79**, S47–S75.
- Donaldson SH & Boucher RC (2003). Update on pathogenesis of cystic fibrosis lung disease. *Curr Opin Pulm Med* **9**, 486–491.
- Fang X, Fukuda N, Barbry P, Sartori C, Verkman AS & Matthay MA (2002). Novel role for CFTR in fluid absorption from the distal airspaces of the lung. *J Gen Physiol* **119**, 199–208.
- Gadsby DC, Nagel G & Hwang TC (1995). The CFTR chloride channel of mammalian heart. *Annu Rev Physiol* **57**, 387–416.
- Gadsby DC & Nairn AC (1999). Control of CFTR channel gating by phosphorylation and nucleotide hydrolysis. *Physiol Rev* **79**, S77–S107.
- Grubb BR, Vick RN & Boucher RC (1994). Hyperabsorption of Na⁺ and raised Ca²⁺-mediated Cl⁻ secretion in nasal epithelia of CF mice. *Am J Physiol* **266**, C1478–C1483.
- Hille B (1992). *Ionic Channels of Excitable Membranes*. Sinauer Associates Inc., Sunderland, MA.
- Hodgkin AL, Huxley AF & Katz B (1952). Measurement of current-voltage relations in the membrane of the giant axon of *Loligo*. *J Physiol* **116**, 424–448.
- Hodgkin AL & Katz B (1949). The effect of sodium ions on the electrical activity of the giant axon of the squid. *J Physiol* **108**, 37–77.
- Horisberger JD (2003). ENaC–CFTR interactions: the role of electrical coupling of ion fluxes explored in an epithelial cell model. *Pflugers Arch* **445**, 522–528.
- Ji HL, Chalfant ML, Jovov B, Lockhart JP, Parker SB, Fuller CM, Stanton BA & Benos DJ (2000). The cytosolic termini of the beta- and gamma-ENaC subunits are involved in the functional interactions between CFTR and ENaC. *J Biol Chem* **275**, 27947–27956.
- Jiang Q, Li J, Dubroff R, Ahn YJ, Foskett JK, Engelhardt J & Kleyman TR (2000). Epithelial sodium channels regulate cystic fibrosis transmembrane conductance regulator chloride channels in *Xenopus* oocytes. *J Biol Chem* **275**, 13266–13274.
- Knowles MR, Gatzky J & Boucher RC (1981). Increased bioelectric potential difference across respiratory epithelia in cystic fibrosis. *N Engl J Med* **305**, 1489–1495.
- Knowles MR, Stutts MJ, Spock A, Fischer N, Gatzky JT & Boucher RC (1983). Abnormal ion permeation through cystic fibrosis respiratory epithelium. *Science* **221**, 1067–1070.
- Ko SB, Shcheynikov N, Choi JY, Luo X, Ishibashi K, Thomas PJ, Kim JY, Kim KH, Lee MG, Naruse S & Muallem S (2002). A molecular mechanism for aberrant CFTR-dependent HCO₃⁻ transport in cystic fibrosis. *EMBO J* **21**, 5662–5672.
- König J, Schreiber R, Voelcker T, Mall M & Kunzelmann K (2001). The cystic fibrosis transmembrane conductance regulator (CFTR) inhibits ENaC through an increase in the intracellular Cl⁻ concentration. *EMBO Rep* **2**, 1047–1051.
- Konstas AA, Koch JP & Korbmayer C (2003). cAMP-dependent activation of CFTR inhibits the epithelial sodium channel (ENaC) without affecting its surface expression. *Pflugers Arch* **445**, 513–521.
- Kunzelmann K (2003). ENaC is inhibited by an increase in the intracellular Cl⁻ concentration mediated through activation of Cl⁻ channels. *Pflugers Arch* **445**, 504–512.
- Kunzelmann K, Mall M, Briel M, Hipper A, Nitschke R, Ricken S & Greger R (1997). The cystic fibrosis transmembrane conductance regulator attenuates the endogenous Ca²⁺ activated Cl⁻ conductance of *Xenopus* oocytes. *Pflugers Arch* **435**, 178–181.
- Lahr TF, Record RD, Hoover DK, Hughes CL & Blazer-Yost BL (2000). Characterization of the ion transport responses to ADH in the MDCK-C7 cell line. *Pflugers Arch* **439**, 610–617.
- Letz B & Korbmayer C (1997). cAMP stimulates CFTR-like Cl⁻ channels and inhibits amiloride-sensitive Na⁺ channels in mouse CCD cells. *Am J Physiol* **272**, C657–C666.
- Lingueglia E, Voilley N, Waldmann R, Lazdunski M & Barbry P (1993). Expression cloning of an epithelial amiloride-sensitive Na⁺ channel. A new channel type with homologies to *Caenorhabditis elegans* degenerins. *FEBS Lett* **318**, 95–99.
- McNicholas CM, Nason MW Jr, Guggino WB, Schwiebert EM, Hebert SC, Giebisch G & Egan ME (1997). A functional CFTR-NBF1 is required for ROMK2–CFTR interaction. *Am J Physiol* **273**, F843–F848.
- Mall M, Bleich M, Greger R, Schreiber R & Kunzelmann K (1998). The amiloride-inhibitable Na⁺ conductance is reduced by the cystic fibrosis transmembrane conductance regulator in normal but not in cystic fibrosis airways. *J Clin Invest* **102**, 15–21.
- Mall M, Hipper A, Greger R & Kunzelmann K (1996). Wild type but not deltaF508 CFTR inhibits Na⁺ conductance when co-expressed in *Xenopus* oocytes. *FEBS Lett* **381**, 47–52.
- Moore JW, Hines M & Harris EM (1984). Compensation for resistance in series with excitable membranes. *Biophys J* **46**, 507–514.
- Nagel G (1999). Differential function of the two nucleotide binding domains on cystic fibrosis transmembrane conductance regulator. *Biochim Biophys Acta* **1461**, 263–274.
- Nagel G (2004). CFTR investigated with the two-electrode voltage-clamp technique: the importance of knowing the series resistance. *J Cystic Fibros* **3**, 109–111.
- Nagel G, Hwang TC, Nastiuk KL, Nairn AC & Gadsby DC (1992). The protein kinase A-regulated cardiac Cl⁻ channel resembles the cystic fibrosis transmembrane conductance regulator. *Nature* **360**, 81–84.

- Nagel G, Szellas T, Grygorczyk R & Barbry P (2001a). Sodium uptake and voltage-clamp experiments in *Xenopus* oocytes provide no evidence for specific regulation of ENaC by CFTR. *Pediatr Pulmonol* **22** (Suppl.), 209.
- Nagel G, Szellas T, Riordan JR, Friedrich T & Hartung K (2001b). Non-specific activation of the epithelial sodium channel by the CFTR chloride channel. *EMBO Rep* **2**, 249–254.
- Park M, Ko SB, Choi JY, Muallem G, Thomas PJ, Pushkin A, Lee MS, Kim JY, Lee MG, Muallem S & Kurtz I (2002). The cystic fibrosis transmembrane conductance regulator interacts with and regulates the activity of the HCO₃⁻ salvage transporter human Na⁺-HCO₃⁻ cotransport isoform 3. *J Biol Chem* **277**, 50503–50509.
- Pilewski JM & Frizzell RA (1999). Role of CFTR in airway disease. *Physiol Rev* **79**, S215–S255.
- Quinton PM (1999). Physiological basis of cystic fibrosis: a historical perspective. *Physiol Rev* **79**, S3–S22.
- Reddy MM, Light MJ & Quinton PM (1999). Activation of the epithelial Na⁺ channel (ENaC) requires CFTR Cl⁻ channel function. *Nature* **402**, 301–304.
- Reddy MM & Quinton PM (2003). Functional interaction of CFTR and ENaC in sweat glands. *Pflugers Arch* **445**, 499–503.
- Reddy MM, Quinton PM, Haws C, Wine JJ, Grygorczyk R, Tabcharani JA, Hanrahan JW, Gunderson KL & Kopito RR (1996). Failure of the cystic fibrosis transmembrane conductance regulator to conduct ATP. *Science* **271**, 1876–1879.
- Reisin IL, Prat AG, Abraham EH, Amara JF, Gregory RJ, Ausiello DA & Cantiello HF (1994). The cystic fibrosis transmembrane conductance regulator is a dual ATP and chloride channel. *J Biol Chem* **269**, 20584–20591.
- Riordan JR (1993). The cystic fibrosis transmembrane conductance regulator. *Annu Rev Physiol* **55**, 609–630.
- Riordan JR, Rommens JM, Kerem B, Alon N, Rozmahel R, Grzelczak Z, Zielenski J, Lok S, Plavsic N & Chou JL (1989). Identification of the cystic fibrosis gene: cloning and characterization of complementary DNA. *Science* **245**, 1066–1073.
- Samaha FF, Rubenstein RC, Yan W, Ramkumar M, Levy DI, Ahn YJ, Sheng S & Kleyman TR (2004). Functional polymorphism in the carboxyl terminus of the alpha-subunit of the human epithelial sodium channel. *J Biol Chem* **279**, 23900–23907.
- Schreiber R, Hopf A, Mall M, Greger R & Kunzelmann K (1999). The first-nucleotide binding domain of the cystic-fibrosis transmembrane conductance regulator is important for inhibition of the epithelial Na⁺ channel. *Proc Natl Acad Sci U S A* **96**, 5310–5315.
- Schreiber R, König J, Sun J, Markovich D & Kunzelmann K (2003). Effects of purinergic stimulation, CFTR and osmotic stress on amiloride-sensitive Na⁺ transport in epithelia and *Xenopus* oocytes. *J Membr Biol* **192**, 101–110.
- Schwiebert EM, Benos DJ, Egan ME, Stutts MJ & Guggino WB (1999). CFTR is a conductance regulator as well as a chloride channel. *Physiol Rev* **79**, S145–S166.
- Schwiebert EM, Egan ME, Hwang TH, Fulmer SB, Allen SS, Cutting GR & Guggino WB (1995). CFTR regulates outwardly rectifying chloride channels through an autocrine mechanism involving ATP. *Cell* **81**, 1063–1073.
- Sheppard DN & Welsh MJ (1999). Structure and function of the CFTR chloride channel. *Physiol Rev* **79**, S23–S45.
- Stutts MJ & Boucher (1999). Cystic fibrosis gene and functions of CFTR. Implications of dysfunctional ion transport for pulmonary pathogenesis. In *Cystic Fibrosis in Adults*, ed. Yankaskas JR & Knowles MR, pp. 3–25. Lippincott-Raven Publishers, Philadelphia.
- Stutts MJ, Canessa CM, Olsen JC, Hamrick M, Cohn JA, Rossier BC & Boucher RC (1995). CFTR as a cAMP-dependent regulator of sodium channels. *Science* **269**, 847–850.
- Stutts MJ, Rossier BC & Boucher RC (1997). Cystic fibrosis transmembrane conductance regulator inverts protein kinase A-mediated regulation of epithelial sodium channel single channel kinetics. *J Biol Chem* **272**, 14037–14040.
- Suaud L, Carattino M, Kleyman TR & Rubenstein RC (2002a). Genistein improves regulatory interactions between G551D-CFTR and the epithelial sodium channel in *Xenopus* oocytes. *J Biol Chem* **277**, 50341–50347.
- Suaud L, Li J, Jiang Q, Rubenstein RC & Kleyman TR (2002b). Genistein restores functional interactions between Delta F508-CFTR and ENaC in *Xenopus* oocytes. *J Biol Chem* **277**, 8928–8933.
- Tarran R, Loewen ME, Paradiso AM, Olsen JC, Gray MA, Argent BE, Boucher RC & Gabriel SE (2002). Regulation of murine airway surface liquid volume by CFTR and Ca²⁺-activated Cl⁻ conductances. *J Gen Physiol* **120**, 407–418.
- Taylor RE, Moore JW & Cole KS (1960). Analysis of certain errors in squid axon voltage clamp measurements. *Biophys J* **1**, 161–202.
- Weinreich F, Riordan JR & Nagel G (1999). Dual effects of ADP and adenylylimidodiphosphate on CFTR channel kinetics show binding to two different nucleotide binding sites. *J Gen Physiol* **114**, 55–70.
- Weinreich F, Wood PG, Riordan JR & Nagel G (1997). Direct action of genistein on CFTR. *Pflugers Arch* **434**, 484–491.
- Yan W, Samaha FF, Ramkumar M, Kleyman TR & Rubenstein RC (2004). Cystic fibrosis transmembrane conductance regulator differentially regulates human and mouse epithelial sodium channels in *Xenopus* oocytes. *J Biol Chem* **279**, 23183–23192.

Acknowledgements

G.N. thanks Professor B. Rossier for the rENaC plasmids, Professor J. Riordan for the hCFTR plasmid, Professor E. Bamberg for generous support and constant encouragement, and Doris Ollig, Saskia Schröder-Lang, and Eva-Verena Bongartz for technical assistance. The support of the Canadian Cystic Fibrosis Foundation (to R.G.) is gratefully acknowledged. The authors thank Ovid Da Silva, Editor, Research Support Office, Research Centre, CHUM, for editing this manuscript.

Author's present address

G. Nagel: Julius-von-Sachs-Institut, University Würzburg, Julius-von-Sachs-Platz 2, D 97082 Würzburg, Germany